tvst

Article

Characterization of the Three Distinct Retinal Capillary Plexuses Using Optical Coherence Tomography Angiography in Myopic Eyes

Qiujian Zhu[1], Xiaoying Xing[2], Mengyu Wang[1], Manhui Zhu[1], Lie Ma[1], You Yuan[1,*], and E. Song[1,*]

[1] Department of Ophthalmology, Lixiang Eye Hospital of Soochow University, Suzhou, China
[2] Suzhou Eye Hospital, Suzhou, China

Correspondence: You Yuan and E. Song, Department of Ophthalmology, Lixiang Eye Hospital of Soochow University, Suzhou 215021, Jiangsu, China. e-mails: yuanyou@suda.edu.cn; songe@suda.edu.cn

Received: September 22, 2019
Accepted: November 19, 2019
Published: March 9, 2020

Keywords: myopia; optical coherence tomography angiography; retina; segmentation; vessel density

Citation: Zhu Q, Xing X, Wang M, Zhu M, Ma L, Yuan Y, Song E. Characterization of the three distinct retinal capillary plexuses using optical coherence tomography angiography in myopic eyes. Trans Vis Sci Tech. 2020;9(4):8, https://doi.org/10.1167/tvst.9.4.8

Purpose: To segment and quantify three distinct retinal capillary plexuses using optical coherence tomography angiography (OCTA) in myopic eyes.

Methods: We analyzed 96 eyes from 62 subjects with myopia (27.76 ± 7.05 years of age) and evaluated 30 normal eyes from 15 subjects (28.33 ± 3.13 years of age) for controls. En face OCTA images generated by AngioPlex (Carl Zeiss; Oberkochen, Germany) were manually segmented by the progressive matching method into superficial, middle, and deep capillary plexuses (SCPs, MCPs, and DCPs, respectively). Estimated positions for each plexus relative to the reference line were calculated. After strict artifact removal and magnification correction, vessel density (VD) and skeleton density (SD) analyses were performed on each capillary plexus.

Results: Myopic eyes were divided into three groups according to their degree of myopia. We defined the relative estimated positions of the MCP outer boundary to the retinal pigment epithelium fit layer as MCP = –89.317 – 0.178 (central retinal thickness) – 0.580 (ganglion cell inner plexiform thickness); the DCP outer boundary was 38.48 ± 6.24 µm below the inner plexiform layer. VDs were significantly higher in the super-high myopia group than in the control and moderate myopia groups for the DCP (all $P < 0.05$). SDs in the SCPs were significantly lower in the high myopia and super-high myopia groups than in the control groups (all $P < 0.001$).

Conclusions: With progressive matching, we segmented three capillary plexuses and defined the relative estimated positions of each capillary plexus to the reference line in myopic eyes. The VD of the DCP increased for more myopic eyes.

Translational Relevance: Our study provides a visual method for OCTA image vascular segmentation for myopic eyes.

Introduction

Uncorrected refractive error is the main cause of visual impairment globally, and myopia is the most common refractive error.[1–3] The prevalence of myopia and high myopia has been increasing globally.[2,4] Even with refractive correction, high myopia can lead to myopic retinopathy, which presents with lacquer crack formation, choroidal neovascularization, and chorioretinal atrophy; these complications are highly associated with retinal vessel morphologic alterations.[5,6] However, due to technical difficulties, previous studies were limited to large retinal vessel analyses, such as color Doppler imaging and the use of fundus cameras.[7,8]

Optical coherence tomography angiography (OCTA) is an advanced ophthalmic imaging technique that can measure the microvasculature structure in different layers of the retina without the use of contrast agents, such as fluorescent dye.[9–11] Because of its high resolution and fast image acquisition time, OCTA is widely used in the detection of vascular changes in various diseases.[12–15]

Because of the limitations of machine software, previous studies of myopia microvascular disease divided retinal vessels into two layers—superficial capillary plexus (SCP) and deep capillary plexus (DCP).[16–18] However, later studies have demonstrated a third capillary plexus, the middle capillary plexus (MCP), which is associated with distinct developmental cues.[19–22] Changes in each of the three distinct capillary plexuses have been described for specific conditions, such as diabetic retinopathy (DR), hyperoxia, and dark adaptation, and it has been demonstrated that each vascular layer undergoes independent changes.[23–26] But, these studies lack definitive evidence for segmentation.

Moreover, the elongation of the axial axis of myopia will lead to changes in the structure of the retina and may also cause changes in the position of the capillary plexuses.[27] To date, we have not found any attempt to segment the three capillary plexuses in OCTA images of patients with myopia.

In this study, we used a progressive matching method to segment the trilaminar capillary plexuses to locate the position of the capillary plexuses in myopic eyes and to describe the changes in the three capillary plexuses in patients with myopia. Our study is an important supplement to previous studies and provides a basis for future myopia research.

Methods

This retrospective study was approved by the Lixiang Eye Hospital of Soochow University Institutional Review Board, adhered to the tenets of the Declaration of Helsinki, and was in compliance with the Health Insurance Portability and Accountability Act. Informed consent was obtained from all subjects, who underwent OCTA imaging between January 2018 and November 2018 in the Department of Ophthalmology at Lixiang Eye Hospital of Soochow University in Suzhou, Jiangsu.

Study Sample

A total of 96 eyes from 62 subjects with myopia were recruited for this study, and a total of 30 normal eyes from 15 subjects were evaluated for controls. All subjects were from a Han Chinese population. Each subject underwent a complete ocular examination, which included slit-lamp biomicroscopy, best-corrected visual acuity), refractive diopter (D) measurement with a Nidek AR-310A autorefractor (Tokyo, Japan), intraocular pressure (IOP) measurement using a Canon TX-20 tonometer (Tokyo, Japan), dilated fundus examination, and axial length (AL) measurement using a Zeiss IOLMaster 500.

The inclusion criteria were best-corrected visual acuity equal to or better than 20/20, spherical equivalent (SE) ≤ -3.00D, normal IOP, no evidence of myopic macular degeneration, and no history of vitreoretinal disease in the study eyes. The SE of the control group ranged from +0.5D to –1.0D. Exclusion criteria included a history of ocular surgery or systemic diseases potentially affecting the eyes, myopic choroidal neovascularization (CNV), poor-quality images with a signal strength less than 8 (maximum of 10), significant motion artifact, or inability to abstain from blinking or movement during image acquisition.

OCTA Imaging

The commercially available Zeiss AngioPlex Cirrus HD-OCT 5000-2328 with optical microangiography image processing (software version 10.0.0.14618) was used for image acquisition. The technical aspects of this device have been previously described in detail.[28] Briefly, this device is capable of scanning at a rate of 68,000 A-scans per second with a light source with a central wavelength of 840 nm and a full-width at half maximum of 90 nm. The 3 × 3-mm^2 optical microangiography scanning mode is achieved by repeating four B-scans at each retinal position in the slow y-axis (245 B-scans at 12.5-µm intervals) with 245 A-scans per B-scan in the fast x-axis.[9] The FAST-Trac function was turned on to minimize the effect of eye motion-related artifacts as previously described.[16,18,28] At least one 3 × 3-mm (759 × 759 pixels) scan centered on the fovea was taken in each eye of interest.

Imaging Segmentation

Segmentation process has been described in detail in a previous study.[29] Briefly, the retinal pigment epithelium (RPE) fit and inner plexiform layer (IPL) were used as the reference line. The DCP and MCP could be captured individually using a thin slab with a certain thickness that was gradually cut upward from the vascularized area of the outer nuclear layer (ONL) (Supplementary Movie S1). We refer to this approach as progressive matching. For the thickness of the DCP and MCP, previous studies have selected a thin slab of 15 µm or 30 µm, but we found that a slab of this thickness could not display an integrated DCP in myopic eyes; thus, we selected a thin slab of 20 µm to segment the DCP following the method of Bonnin.[26,30,31] The process of capture is detailed in Figures 1 and 2, and this process was performed twice with RPE fit and IPL as reference lines. We then defined the SCP as a slab

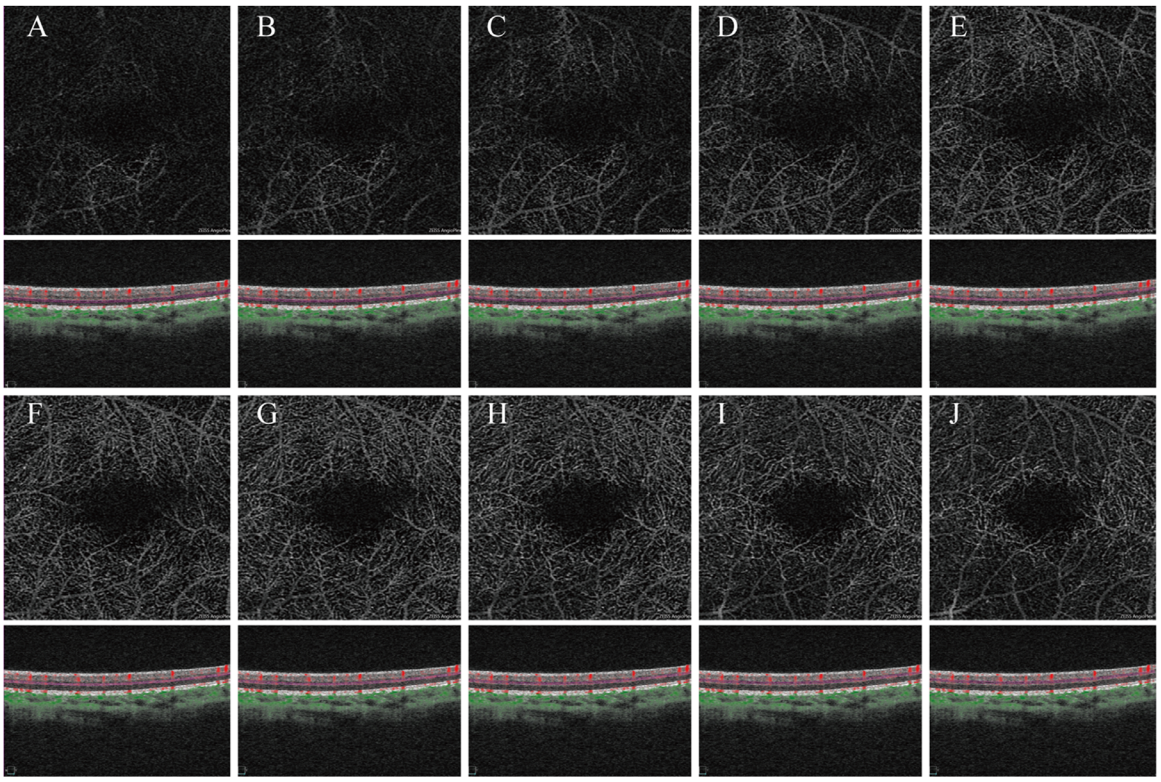

Figure 1. Segmentation of DCPs on OCTA. **(A–J)** A 20-µm-thin slab captures DCPs gradually inward from the avascular zone of the outer nuclear layer at 6-µm intervals until the continuous capillary plexus is disconnected. Image (G) contained the most complete vascular structure and was considered to be the DCP. The red lines on cross-sectional OCTA show the segmentation boundaries for each layer.

from 0 µm beneath the inner limiting membrane (ILM) to 70 µm beneath the ILM.[20,29,32] The results of the three retinal capillary plexuses are shown in Supplementary Figure S2.

The manual "Remove Projections" option in the AngioPlex software was activated to reduce projection artifacts in the lower layers for MCP and DCP analyses.[33] We obtained the MCP and DCP after removal of the decorrelation tail artifact (MCP-re and DCP-re, respectively); however, the effect was better for the DCP than for the MCP (Supplementary Fig. S2). Therefore, we used the minimum projection method in ImageJ version 1.52a (http://imagej.nih.gov/ij/; National Institutes of Health, Bethesda, MD) to remove the decorrelation tail artifact of the MCP. In short, the SCP and MCP were fused into a stack using ImageJ, the minimum projection map was generated using *z*-projection, and, finally, the artifact-removed MCP was obtained by subtracting the minimum projection map with MCP (Fig. 3).

En Face Imaging Analysis

En face OCTA images were analyzed with ImageJ version 1.50i. Fundus photography and OCTA magnification is different in myopic eyes due to axial elongation; hence, proper magnification correction is required for evaluating the dimensional information of the retina. Bennett's formula, $t = p \times q \times s$ (where t as the real scan length, p is the magnification factor determined by the OCT imaging system camera, q is the magnification factor related to the eye, and s is the original measurement from the OCT image), was used to adjust the image magnification based on the AL.[13,14,27,34] The reference AL for the OCT imaging system camera is 24.46 mm; as a result, the scaling factor $(p \times q) = 3.3823 \times 0.0130623(\text{AL} - 1.82)$. Because high-myopia images would change pixel size after adjusting for the scaling factor from Bennett's formula, they were trimmed to the original pixel size (759 × 759 pixels) in the corrected image (Fig. 4).

To calculate vessel density (VD) and skeleton density (SD), we thresholded the face image of each capillary plexus according to the gray value of the foveal avascular zone, generating a binarized black-and-white slab. VD was calculated as the proportion of detected OCTA signal (white pixels in the binarized image) to total pixels. Then, a skeletonized slab was created on this slab, representing a vessel with a width of 1 pixel. SD was defined as the ratio of the length

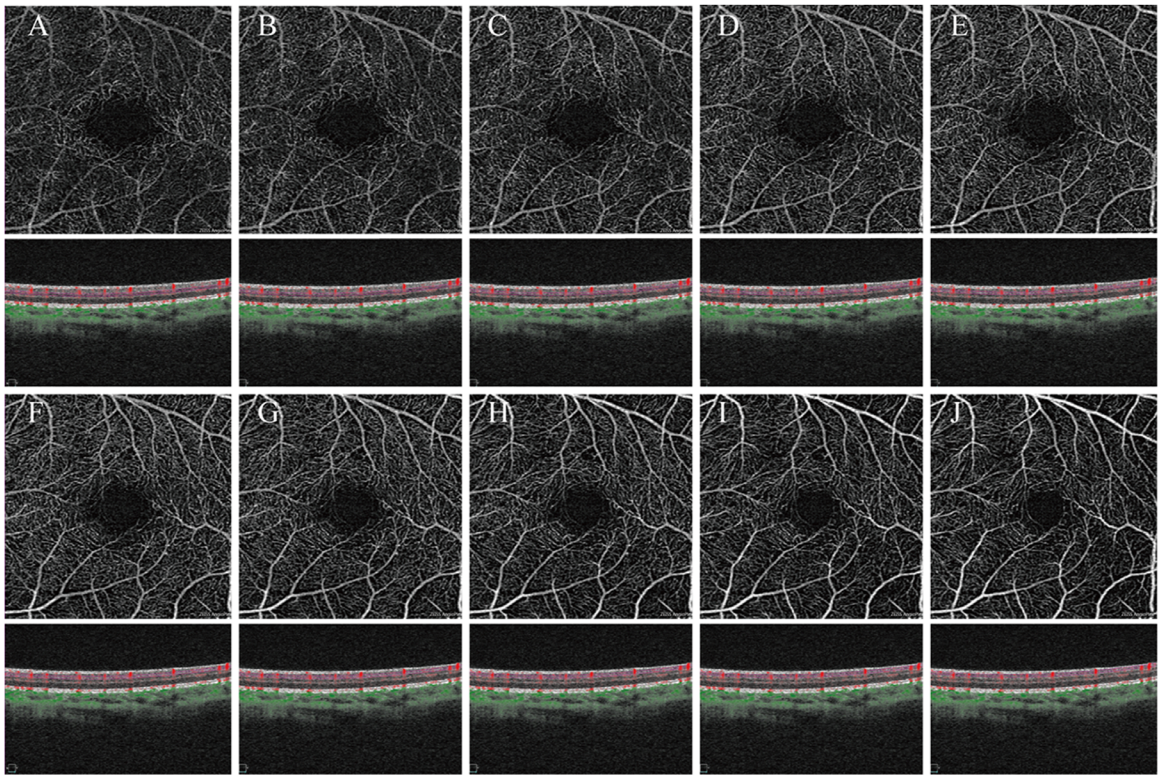

Figure 2. Segmentation of MCPs on OCTA. **(A–J)** A 30-µm-thin slab continued to move upward at an interval of 6 µm until the vascular structure details began to disappear to capture the MCP. Image (G) contained the most complete vascular structure details and was considered to be the MCP. The red lines on cross-sectional OCTA show the segmentation boundaries for each layer.

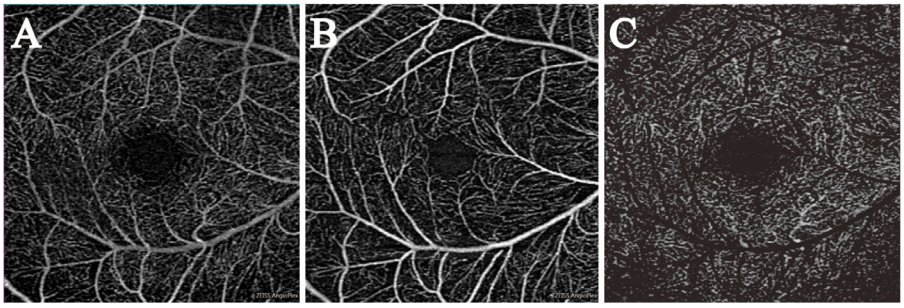

Figure 3. Removal of the decorrelation tail artifact in the MCP using the minimum-projection method of ImageJ. The (A) MCP and (B) SCP were fused into a stack using ImageJ; the minimum projection map was generated using *z*-projection. (C) Finally, the MCP-re was obtained by subtracting the minimum projection map with the MCP.

of the vascular skeleton to the total area of the image (Supplementary Fig. S3). A similar approach has been described in detail in many previous reports.[11,17,35]

OCT Analysis

In addition, macular tomographic OCT was scanned in each eye (macular cube 512 × 128 scan), and central retinal thickness (CRT) and ganglion cell inner plexiform thickness (GCT) were measured using built-in software on the Cirrus device. CRT was defined as the distance between the ILM and RPE within 1 mm of the fovea, and GCT was defined as the thickness between the upper edge of the ganglion cell layer and the lower edge of the inner plexiform layer.

Statistical Analysis

Statistical analysis was performed using SPSS 18.0 (IBM; Armonk, NY). The SE of refractive error was calculated as the spherical dioptric power plus one-half of the cylindrical dioptric power. For all tests,

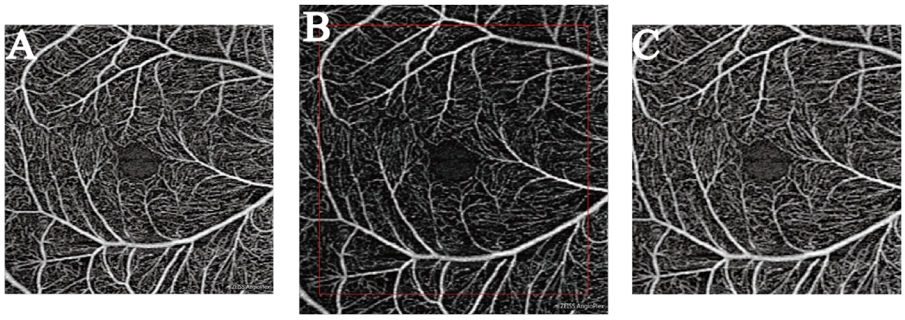

Figure 4. Magnification correction of optical coherence tomography angiography image. The original image (A) (759 × 759 pixels) was magnified 1.15× according to the axial length (AL = 27.90 mm) to create the magnified image (B) (873 × 873 pixels), which was further cropped to the size of the original image (C) (759 × 759 pixels).

Table 1. Characteristics among the Different Groups

Variables	Control	Moderate Myopia	High Myopia	Super-High Myopia	*F*	*P*
Number of eyes	30	14	57	25		
Age (y)	28.33 ± 3.08	29.86 ± 8.19	27.56 ± 6.44	26.52 ± 6.90	0.988	0.401
Mean AL (mm)	23.28 ± 0.67	24.79 ± 0.70	26.72 ± 1.17	27.28 ± 1.03	102.306	<0.001**
Mean SE (D)	–0.18 ± 0.61	–4.07 ± 0.83	–7.44 ± 0.82	–10.18 ± 1.11	754.51	<0.001**
Mean CRT (μm)	240.33 ± 21.26	244.86 ± 12.83	251.12 ± 20.23	249.80 ± 14.49	2.369	0.074
Mean GCT (μm)	85.97 ± 3.32	79.93 ± 4.98	77.28 ± 5.71	74.32 ± 5.48	27.832	<0.001**

Data are expressed as the mean ± standard deviation; one-way analysis of variance.
**$P < 0.01$.

P values < 0.05 were considered statistically significant. All data are reported as means and standard deviations. One-way analysis of variance was used for overall effects among the four groups, and the least significant difference test was used for post hoc analyses. Pearson's correlations were used to study the association between the location of each capillary plexus and the AL and SE. A linear regression model (stepwise method) was used for multivariate analyses and to calculate the location of the MCP and DCP outer boundaries.

Results

Subject Demographics and Clinical Characteristics

The mean ages of the myopia subjects and control subjects were 27.76 ± 7.05 years and 28.33 ± 3.13 years, respectively. The eyes of the myopia subjects were subsequently divided into groups according to their degree of myopia: 14 eyes were included in the moderate myopia group (–6.00D < SE ≤ –3.00 D), 57 eyes were included in the high myopia group (–9.00D < SE ≤ –6.00D), and 25 eyes were included in the super-high myopia group (SE ≤ –9.00D). The subjects' characteristics are shown in Table 1. The CRTs in the control (240.33 ± 21.26 μm), moderate myopia (244.86 ± 12.83 μm), high myopia (251.12 ± 20.23 μm), and super-high myopia (249.80 ± 14.49 μm) groups were not significantly different ($P = 0.074$) (Table 1). The GCTs in the control (85.97 ± 3.32 μm), moderate myopia (79.93 ± 4.98 μm), high myopia (77.28 ± 5.71 μm), and super-high myopia (74.32 ± 5.48 μm) groups were significantly different ($P < 0.001$) (Table 1).

Localization of MCP and DCP In Four Groups

If RPE fit was used as the reference line, the outer boundaries of the MCP were 183.30 ± 13.22 μm, 179.93 ± 7.32 μm, 179.30 ±9.31 μm, and 175.76 ± 9.22 μm above the reference line in the control, moderate myopia, high myopia, and super-high myopia groups, respectively. The outer boundaries of the DCP were 137.60 ± 11.42 μm, 135.14 ± 6.05 μm, 134.32 ± 8.07 μm, and 131.28 ± 8.80 μm above the reference line for the four groups, respectively. The MCP and DCP outer boundaries were not significantly different among the groups ($P = 0.061$ and $P = 0.553$, respectively) (Table 2). If the IPL was used as the reference line, the outer boundaries of the MCP were 15.70 ± 8.03 μm, 10.43 ± 5.98 μm, 9.91 ± 7.27 μm, and 8.52 ± 6.42 μm above the line for the four groups, respectively

Table 2. Position of the Outer Boundary of the MCP and DCP Relative to the IPL and RPE Fit

Capillary	Plexus	Control	Moderate Myopia	High Myopia	Super-High Myopia	*F*	*P*
MCP	Mean RPE fit (μm)	−183.30 ± 13.22	−179.93 ± 7.32	−179.30 ± 9.31	−175.76 ± 9.22	2.525	0.061
	IPL (μm)	−15.70 ± 8.03	−10.43 ± 5.98	−9.91 ± 7.27	−8.52 ± 6.42	5.749	0.001**
DCP	Mean RPE fit (μm)	−137.60 ± 11.42	−135.14 ± 6.05	−134.32 ± 8.07	−131.28 ± 8.80	2.308	0.080
	Mean IPL (μm)	37.63 ± 7.04	38.43 ± 6.15	38.19 ± 6.46	39.16 ± 5.97	0.259	0.855

Data are expressed as the mean ± standard deviation; one-way analysis of variance. The minus sign indicates above the reference line.

**$P < 0.01$.

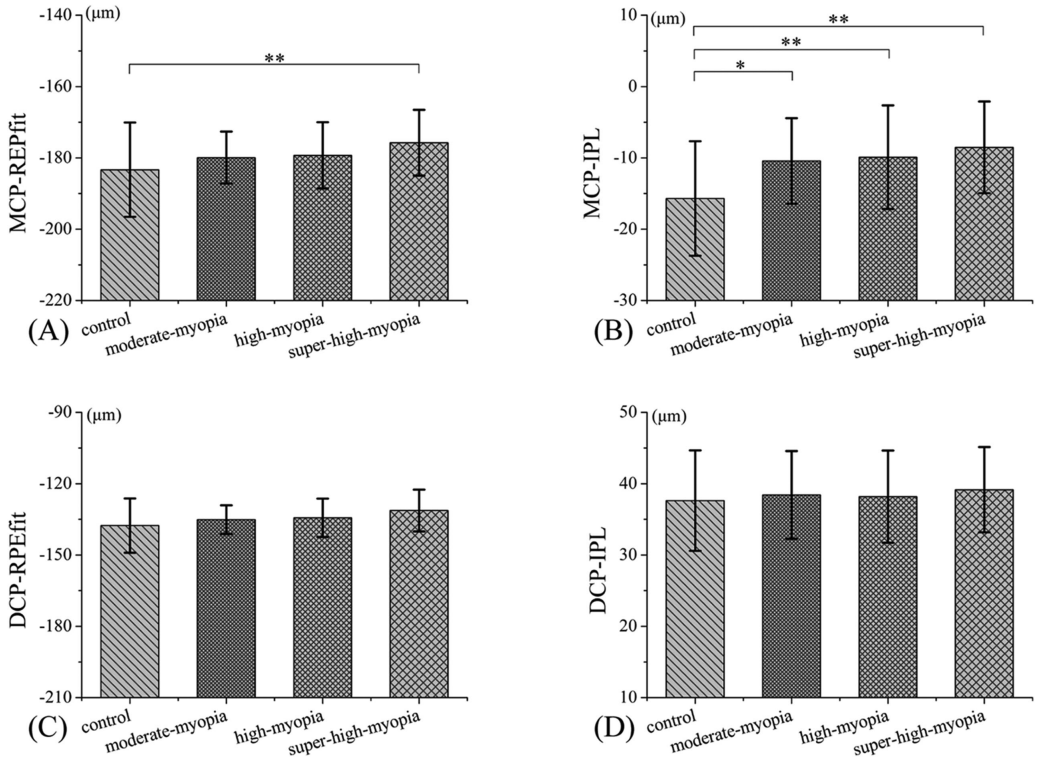

Figure 5. Position of the outer boundary of the MCP and DCP relative to RPE fit and IPL among the four groups. (A) The MCP position with RPE fit as the reference line. (B) The MCP position with IPL as the reference line. (C) The DCP position with RPE fit as the reference line. (D) The DCP position with IPL as the reference line. The position of the MCP relative to the RPE fit was higher in the super-high myopia group than in the control group. The position of the MCP relative to the IPL was higher in the control group than in the three myopia groups. The DCP position did not show any differences between any two groups. The minus sign indicates above the reference line; post hoc least significant difference test. *$P < 0.05$; **$P < 0.01$.

($P = 0.001$) (Table 2). The results for the DCP were 37.63 ± 7.04 μm, 38.43 ± 6.15 μm, 38.19 ± 6.46 μm, and 39.16 ± 5.97 μm below the line for the four groups, respectively ($P = 0.855$) (Table 2).

The position of the MCP relative to RPE fit was higher in the super-high myopia group than in the control group ($P < 0.001$) (Fig. 5). The position of the MCP relative to the IPL was higher in the control group than in the three myopia groups ($P = 0.036$, $P = 0.006$, and $P = 0.003$) (Fig. 5). The DCP position did not show any significant difference between any two groups.

Multivariate Linear Regression Analysis

We performed multivariate linear regression analyses to investigate the factors affecting the relative position. If RPE fit was used as the reference line, the position of the MCP was affected by GCT and CRT (all $P < 0.01$), and the position of the DCP was affected by GCT ($P = 0.009$) (Table 3). If the IPL was used as the reference line, the position of the MCP was affected by AL and CRT (all $P = 0.029$ and $P = 0.001$, respectively) (Table 3). Furthermore, only the

Table 3. Linear Regression Analysis of Factors Affecting the Relative Position

Factor	Model 1 Coefficient†	*P*	Model 2 Coefficient†	*P*
Mean MCP relative to RPE fit	Adjusted $R^2 = 0.235$		Adjusted $R^2 = 0.228$	
Mean AL	0.221	0.092	—	—
Mean SE	0.112	0.342	—	—
Mean CRT	–0.395	<0.001**	–0.352 (–0.178)	<0.001**
Mean GCT	–0.306	0.004**	–0.369 (–0.580)	<0.001**
MCP relative to IPL	Adjusted $R^2 = 0.094$		Adjusted $R^2 = 0.102$	
Mean AL	0.313	0.029*	0.225 (1.163)	0.029*
Mean SE	0.141	0.275	—	—
Mean CRT	–0.342	0.001**	–0.335 (–0.128)	0.001**
Mean GCT	–0.009	0.934	—	—
DCP relative to RPE fit	Adjusted $R^2 = 0.098$		Adjusted $R^2 = 0.061$	
Mean AL	0.277	0.053	—	—
Mean SE	0.106	0.408	—	—
Mean CRT	–0.222	0.032*	—	—
Mean GCT	–0.186	0.100	–0.267 (–0.372)	0.009**
DCP relative to IPL	Adjusted $R^2 = 0.081$		—	
Mean AL	0.382	0.009**	—	—
Mean SE	0.127	0.328	—	—
Mean CRT	–0.181	0.083	—	—
Mean GCT	0.318	0.006**	—	—

Model 1, input; Model 2, stepwise.
*$P < 0.05$.
**$P < 0.01$.
†Standardized coefficient; unstandardized coefficient is in parentheses.

Table 4. Microvascular Parameters of Three Capillary Plexuses in the Four Groups

Capillary	Plexus	Control	Moderate Myopia	High Myopia	Super-High Myopia	*F*	*P*
SCP	VD (%)	32.97 ± 3.90	30.95 ± 4.39	32.46 ± 4.57	32.70 ± 6.02	0.613	0.608
	SD (mm^{-1})	14.45 ± 1.51	13.52 ± 1.75	12.90 ± 1.75	12.75 ± 2.16	5.936	<0.001**
MCP	VD (%)	42.27 ± 3.27	39.89 ± 7.36	41.24 ± 5.32	42.94 ± 6.79	1.166	0.326
	SD (mm^{-1})	18.87 ± 1.31	17.65 ± 2.77	16.82 ± 2.12	17.09 ± 2.39	6.566	<0.001**
MCP-re	VD (%)	29.43 ± 2.79	29.34 ± 4.06	30.61 ± 3.49	31.96 ± 4.02	2.868	0.039*
	SD (mm^{-1})	14.10 ± 1.26	14.31 ± 1.80	14.17 ± 1.40	14.78 ± 1.71	1.178	0.321
DCP	VD (%)	32.57 ± 3.55	31.56 ± 4.67	35.98 ± 5.83	37.72 ± 6.41	6.711	<0.001**
	SD (mm^{-1})	15.62 ± 1.48	14.98 ± 1.75	15.37 ± 2.21	15.71 ± 2.37	0.484	0.694
DCP-re	VD (%)	28.94 ± 2.64	28.67 ± 4.56	32.16 ± 5.91	34.69 ± 5.79	7.410	<0.001**
	SD (mm^{-1})	13.85 ± 1.13	13.53 ± 1.90	13.88 ± 2.35	14.53 ± 2.20	0.919	0.434

Data are expressed as the mean ± standard deviation; one-way analysis of variance.
*$P < 0.05$.
**$P < 0.01$.

MCP relative to RPE fit had a good degree of fit (adjusted $R^2 = 0.228$) (Table 3). Therefore, we used the regression equation MCP = –89.317 – 0.178CRT – 0.580GCT, with RPE fit as the reference line. Table 3 shows the detailed results of the linear regression analyses.

Microvascular Changes in the Four Groups

VDs of the MCP-re, DCP, and DCP-re were significantly different among the four groups (all $P < 0.05$) (Table 4). In the super-high myopia group, VD was significantly higher than in the control and moderate

Table 5. Correlations of Ocular Parameters with Microvascular Parameters

		SCP		MCP		MCP-re		DCP		DCP-re	
Parameter	Correlation	VD	SD	VD	SD	VD	SD	VD	SD	VD	SD
Mean AL	*r*	0.052	−0.242	0.064	−0.239	0.091	−0.123	0.209	−0.082	0.272	0.020
	P	0.612	0.017*	0.537	0.019*	0.379	0.233	0.041*	0.426	0.007**	0.845
Mean SE	*r*	−0.116	0.121	−0.178	0.061	−0.202	−0.080	−0.315	−0.104	−0.364	−0.183
	P	0.261	0.242	0.082	0.556	0.048*	0.441	0.002**	0.315	<0.001**	0.074
Mean GCT	*r*	0.128	0.227	0.143	0.257	0.090	0.121	0.144	0.283	0.035	0.127
	P	0.214	0.026*	0.165	0.012*	0.384	0.241	0.161	0.005**	0.736	0.216
Mean CRT	*r*	0.085	−0.037	0.166	0.072	0.253	0.186	0.314	0.253	0.324	0.269
	P	0.409	0.717	0.106	0.485	0.013*	0.070	0.002**	0.013*	0.001**	0.008**

*$P < 0.05$.
**$P < 0.01$.

myopia groups for the MCP-re, DCP, and DCP-re (all $P < 0.05$) (Fig. 6). In the SCP and MCP, the SDs of the control group were significantly higher than those of the high myopia and super-high myopia groups (all $P < 0.001$) (Fig. 6). In the MCP-re, DCP, and DCP-re, the SDs were not significantly different among the four groups (all $P > 0.05$) (Table 4).

Correlation Analysis

To determine the factors associated with the parameters of the microvasculature in all myopia subjects, we performed correlation analyses. In patients with myopia, the SDs of the SCP and MCP were weakly negatively correlated with the AL ($P = 0.017$ and $P = 0.019$, respectively) and were positively correlated with GCT ($P = 0.026$ and $P = 0.012$, respectively) (Table 5). The VDs in the DCP and DCP-re were positively correlated with AL and negatively correlated with SE (all $P < 0.05$) (Table 5). The VD of MCP-re was slightly negatively correlated with SE ($P = 0.048$) (Table 5). In addition, the VDs and SDs in the DCP and DCP-re were all positively correlated with CRT (all $P < 0.01$), and SD in the DCP was positively correlated with GCT ($P = 0.005$) (Table 5). VD in the MCP-re was positively correlated with CRT ($P = 0.013$), and SD in the MCP was positively correlated with GCT ($P = 0.012$) (Table 5).

Discussion

Using a customized manual segmentation we refer to as progressive matching, we have successfully used OCTA to distinguish the three distinct retinal capillary plexuses in myopic eyes. After magnification correction and artifact removal, we initially analyzed the VDs and SDs of the three capillary plexuses in subjects with myopia.

We believe that RPE fit is a reasonable reference line for the description of the location of capillary plexuses because, as mentioned before, in the AngioPlex platform the IPL is not a real anatomical location but an approximate line calculated by the ILM and RPE fit, but given that previous studies have used the IPL as a reference line[9,30] we still included the IPL in this study.

In this study, the MCP was mostly located near the IPL, and the DCP was mostly located near the OPL, a finding that is compatible with most previous studies.[9,19,26,30,36–38] The outer boundaries of the MCP were 183.30 ± 13.22 µm, 179.93 ± 7.32 µm, 179.30 ± 9.31 µm, and 175.76 ± 9.22 µm above RPE fit in the control, moderate myopia, high myopia, and super-high myopia groups, respectively. The position of the MCP was lower in the super-high myopia group than in the control group. Liu et al.[27] and Ye et al.[39] found that the Henle fiber layer and ONL, which comprise the largest portion of the retina, became thinner with the progression of myopia, and the inner nuclear layer showed the same changes. This change may explain why the position of the MCP declined. Alternatively, multivariate analysis revealed that both GCT and CRT had an effect on the location of the MCP. Thus, we used the regression equation MCP = –89.317 – 0.178CRT – 0.580GCT with RPE fit as the reference line. This means that, for each micron increase in GCT, the MCP location will be elevated by 0.580 µm, and for each micron increase in CRT the MCP location will be elevated by 0.178 µm.

The outer boundaries of the DCP were 137.60 ± 11.42 µm, 135.14 ± 6.05 µm, 134.32 ± 8.07 µm, and 131.28 ± 8.80 µm above the RPE fit in the control, moderate myopia, high myopia, and super-high myopia

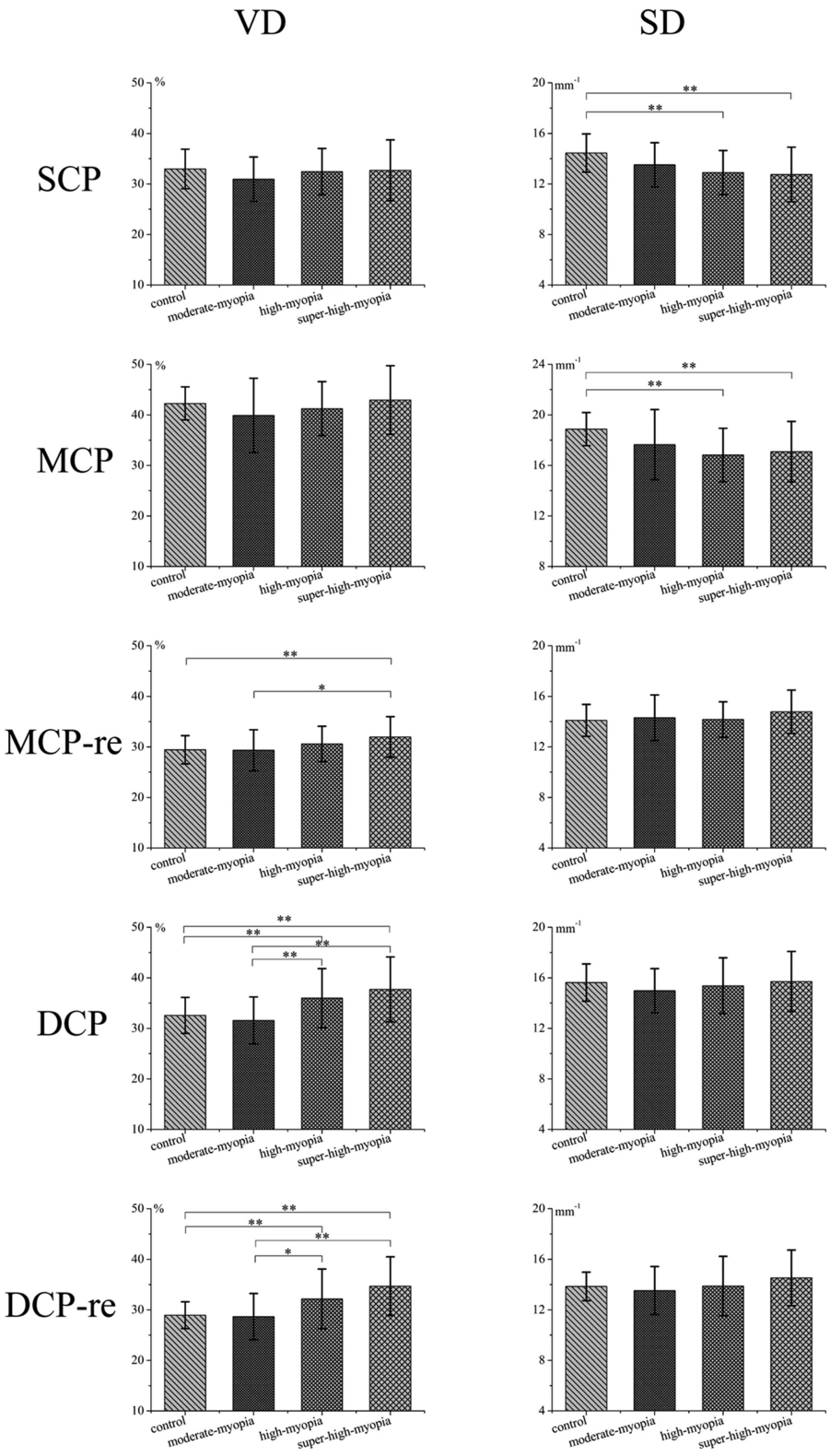

Figure 6. Microvascular changes in the four groups. In the super-high myopia group, VD was significantly higher than that in the control and moderate-myopia groups for the MCP-re, DCP, and DCP-re. In the SCP and MCP, the SDs of the control group were significantly higher than those of the high-myopia and super-high myopia groups; in the MCP-re and DCP, the SDs were not statistically different among the four groups. Post hoc least significant difference test. $^{*}P < 0.05$; $^{**}P < 0.01$.

groups, respectively. Although the location of the DCP also decreased with the progression of myopia, none of these values was significant. This lack of a difference may be related to thickening of the outer plexiform layer (OPL) as myopia progresses.[27,39] Although the thickness of the Henle fiber layer and ONL decreases with the progression of myopia, the thickening of the OPL counteracts some of these effects, and the reduction in the inner nuclear layer, which affects the location of the MCP, does not influence the location of the DCP.

If the IPL was taken as the reference line, the position of the MCP would gradually approach the reference line with the progression of myopia, but the linear regression analysis indicated that its fitting degree was low (adjusted $R^2 = 0.102$). Therefore, the use of the IPL as the reference line was not suitable to provide the regression equation. Interestingly, the location of the DCP relative to the IPL was surprisingly similar in the four groups and was not affected by myopia.

In summary, in subjects with myopia, the position of the MCP, whether using the RPE fit or IPL as a reference line, will be affected by myopia. Therefore, the method of fixed-distance segmentation with a reference line is not suitable, and the progressive matching method is a more reasonable segmentation method. We also used a simpler regression equation. However, if the IPL is used as a reference line, the location of the DCP is relatively fixed, approximately 38.48 ± 6.24 µm below the IPL.

Microvascular changes in myopia have long been a controversial topic. Venkatesh et al.[40] found that the VDs of the DCPs were positively correlated with AL and negatively correlated with SE, whereas the VDs of superficial capillary plexuses were independent of both AL and SE. By contrast, Mo et al.[41] concluded that the VDs of SCPs in highly myopic eyes were lower than those in control eyes, and the VDs of DCPs in myopic eyes were not significantly different from those in control eyes. In addition, Al-Sheikh et al.[12] found that VDs were lower in both the SCPs and DCPs in highly myopic eyes than in control eyes. Wang et al.[42] reported no significant differences in parafoveal superficial VDs among the four myopia groups; however, all of their studies were based on the calculation of VDs by built-in software in an instrument that had not been previously corrected for magnification, thus resulting in under- or overestimation of the measurement of VD. This may be a significant factor that explains why conflicting findings have been reported in previous studies. Li et al.[13] and Yang et al.[14] also studied microvascular morphology in highly myopic eyes after magnification correction, and they found that the fractal dimension in both superficial and deep layers was lower in highly myopic eyes than in control eyes.

In this study, we found that SDs of SCPs and MCPs were significantly lower in the high myopia and super-high myopia groups than in the control group. The process of calculating SDs was similar to that for FDs and involved only the one-dimensional morphology of vessels, which may explain why Li et al.[13] and Yang et al.[14] came to their conclusions. However, after artifact removal, there was no significant difference in the SDs of the MCP-re among the groups, which may be caused by the interference of the SCP with the MCP, so artifact removal is necessary for the MCP. Meanwhile, we found that the SD of the DCP did not differ significantly among the four groups regardless of artifact removal. This result is not consistent with those of Li et al.[13] and Yang et al.[14] and may be caused by the different calculation strategy. For artifact removal for DCPs, we used the algorithm provided by the instrument, whereas Li et al.[13] and Yang et al.[14] considered that all the vessels larger than 25 µm were artifacts and were thus removed, which may lead to misinterpretation of their results.[13,14]

However, in DCPs, with or without artifact removal, the VDs in the super-high myopia group and high myopia group were significantly higher than those in the control and moderate myopia groups. Additionally, for the MCP-re, the VD in the super-high myopia group revealed the same result. In addition, VDs in the DCP and DCP-re were positively correlated with the AL and negatively correlated with SE. These results suggest that with the aggravation of myopia, the VD of deep and middle capillary plexuses may increase, and the changes in the DCPs seem to occur earlier than those in the middle capillary plexuses. This finding came as a surprise to us, and at present we cannot accurately explain this phenomenon. The current study found maximally dilated DCPs and decreased skeletonized-density SCPs in dark adaptation, in order to maximize oxygen delivery to the highly metabolically active dark-adapted photoreceptors.[25] This change was highly consistent with our study. In animal models, the major oxygen-consuming layers are the inner segments of the photoreceptors, the outer plexiform layer, and the deeper region of the inner plexiform layer, and these layers are most vulnerable to hypoxic insult.[43] Al-Sheikh et al.[12] supported decreased choroidal blood flow in patients with high myopia, and we suspect that it may be a compensatory response caused by a decreased SCP and choroid blood flow status to ensure oxygen supply to the high oxygen-consuming layers.

Moreover, our findings may explain an interesting phenomenon. Epidemiological studies have shown that

myopia, especially high myopia, is a protective factor for DR.[44–46] Retinal hypoxia has been established as a major factor contributing to the development of DR.[47,48] Studies have reported that the adjusted flow index of MCP and DCP decreased significantly, while the adjusted flow index of the SCP was unchanged or increased during the progression of DR, suggesting that the deep blood flow status is closely related to the occurrence and development of DR.[23,49] The VD of the DCPs is significantly increased in subjects with high myopia, and hypoxia is obvious in DR; therefore, patients with high myopia may have better adaptability to diabetic changes.

This research had several limitations. First, we used the AngioPlex platform instead of the AngioVue platform used by most studies, and whether the difference between the two has an impact on the results warrants further investigation. Second, because our subjects were all young Han Chinese, our study was minimally affected by confounding factors, which is not conducive to generalization of the results. We will add more types of subjects in the follow-up study. Third, in the previous study, we found that the artifact removal method for the MCP that is provided by the AngioPlex was not ideal,[29] so we used the minimum projection method for artifact removal, which may be the best solution currently available, but part of the blood flow signal is lost when an artifact is removed. We expect more advanced technology and equipment algorithms in the future, such as the recently commercially available widefield swept-source OCTA platforms.

In conclusion, our progressive matching method allowed us to successfully segment the three capillary plexuses in subjects with myopia and to perform localization analysis. Moreover, after strict artifact removal and magnification correction, we found that with the aggravation of myopia, the SD of the SCP decreased but the VDs of the MCP and DCP increased.

Acknowledgments

We thank Haixiang Xiao for his help in data collection.

Supported by Suzhou Science and Technology Bureau (nos. SS201758 and SYS2018004), Jiangsu Distinguished Medical Experts Program (no. 2016), Gusu Health Leading Talent Plan (grant no. 025), and the Technology Program of Soochow City (no. SYS201375).

Disclosure: **Q. Zhu,** None; **X. Xing,** None; **M. Wang,** None; **M. Zhu,** None; **L. Ma,** None; **Y. Yuan,** None; **E. Song,** None

* YY and ES contributed equally to this work.

References

1. Bourne RR, Stevens GA, White RA, et al. Causes of vision loss worldwide, 1990-2010: a systematic analysis. *Lancet Glob Health*. 2013;1:e339–e349.
2. Holden BA, Fricke TR, Wilson DA, et al. Global prevalence of myopia and high myopia and temporal trends from 2000 through 2050. *Ophthalmology*. 2016;123:1036–1042.
3. Fricke TR, Jong M, Naidoo KS, et al. Global prevalence of visual impairment associated with myopic macular degeneration and temporal trends from 2000 through 2050: systematic review, meta-analysis and modelling. *Br J Ophthalmol*. 2018;102:855–862.
4. Morgan IG, Ohno-Matsui K, Saw SM. Myopia. *Lancet*. 2012;379:1739–1748.
5. Li H, Mitchell P, Rochtchina E, et al. Retinal vessel caliber and myopic retinopathy: the blue mountains eye study. *Ophthalmic Epidemiol*. 2011;18:275–280.
6. Kim YM, Yoon JU, Koh HJ. The analysis of lacquer crack in the assessment of myopic choroidal neovascularization. *Eye (Lond)*. 2011;25:937–946.
7. Benavente-Pérez A, Hosking SL, Logan NS, et al. Ocular blood flow measurements in healthy human myopic eyes. *Graefes Arch Clin Exp Ophthalmol*. 2010;248:1587–1594.
8. Azemin MZC, Daud NM, Ab Hamid F, et al. Influence of refractive condition on retinal vasculature complexity in younger subjects. *Sci World J*. 2014;2014:783525–783525.
9. Nesper PL, Fawzi AA. Human parafoveal capillary vascular anatomy and connectivity revealed by optical coherence tomography angiography. *Invest Ophthalmol Vis Sci*. 2018;59:3858–3867.
10. Tan ACS, Tan GS, Denniston AK, et al. An overview of the clinical applications of optical coherence tomography angiography. *Eye (Lond)*. 2017;32:262–286.
11. Kashani AH, Chen CL, Gahm JK, et al. Optical coherence tomography angiography: a comprehensive review of current methods and clinical applications. *Prog Retin Eye Res*. 2017;60:66–100.
12. Al-Sheikh M, Phasukkijwatana N, Dolz-Marco R, et al. Quantitative OCT angiography of

the retinal microvasculature and the choriocapillaris in myopic eyes. *Invest Ophthalmol Vis Sci*. 2017;58:2063–2069.
13. Li M, Yang Y, Jiang H, et al. Retinal microvascular network and microcirculation assessments in high myopia. *Am J Ophthalmol*. 2017;174:56–67.
14. Yang Y, Wang J, Jiang H, et al. Retinal microvasculature alteration in high myopia. *Invest Ophthalmol Vis Sci*. 2016;57:6020–6030.
15. Miyata M, Ooto S, Hata M, et al. Detection of myopic choroidal neovascularization using optical coherence tomography angiography. *Am J Ophthalmol*. 2016;165:108–114.
16. Durbin MK, An L, Shemonski ND, et al. Quantification of retinal microvascular density in optical coherence tomographic angiography images in diabetic retinopathy. *JAMA Ophthalmol*. 2017;135:370–376.
17. Kim AY, Chu Z, Shahidzadeh A, et al. Quantifying microvascular density and morphology in diabetic retinopathy using spectral-domain optical coherence tomography angiography. *Invest Ophthalmol Vis Sci*. 2016;57:OCT362–OCT370.
18. Gao SS, Jia Y, Zhang M, et al. Optical coherence tomography angiography. *Invest Ophthalmol Vis Sci*. 2016;57:OCT27–OCT36.
19. Tan PE, Yu PK, Balaratnasingam C, et al. Quantitative confocal imaging of the retinal microvasculature in the human retina. *Invest Ophthalmol Vis Sci*. 2012;53:5728–5736.
20. Lutty GA, McLeod DS. Development of the hyaloid, choroidal and retinal vasculatures in the fetal human eye. *Prog Retin Eye Res*. 2018;62:58–76.
21. Selvam S, Kumar T, Fruttiger M. Retinal vasculature development in health and disease. *Prog Retin Eye Res*. 2018;63:1–19.
22. Usui Y, Westenskow PD, Kurihara T, et al. Neurovascular crosstalk between interneurons and capillaries is required for vision. *J Clin Invest*. 2015;125:2335–2346.
23. Onishi AC, Nesper PL, Roberts PK, et al. Importance of considering the middle capillary plexus on OCT angiography in diabetic retinopathy. *Invest Ophthalmol Vis Sci*. 2018;59:2167–2176.
24. Hagag AM, Pechauer AD, Liu L, et al. OCT angiography changes in the 3 parafoveal retinal plexuses in response to hyperoxia. *Ophthalmol Retina*. 2018;2:329–336.
25. Nesper PL, Lee HE, Fayed AE, et al. Hemodynamic response of the three macular capillary plexuses in dark adaptation and flicker stimulation using optical coherence tomography angiography. *Invest Ophthalmol Vis Sci*. 2019;60:694–703.
26. Park JJ, Soetikno BT, Fawzi AA. Characterization of the middle capillary plexus using optical coherence tomography angiography in healthy and diabetic eyes. *Retina*. 2016;36:2039–2050.
27. Liu X, Shen M, Yuan Y, et al. Macular thickness profiles of intraretinal layers in myopia evaluated by ultrahigh-resolution optical coherence tomography. *Am J Ophthalmol*. 2015;160:53.e2–61.e2.
28. Rosenfeld PJ, Durbin MK, Roisman L, et al. ZEISS AngioPlex spectral domain optical coherence tomography angiography: technical aspects. *Dev Ophthalmol*. 2016;56:18–29.
29. Zhu Q, Xing X, Zhu M, et al. A new approach for the segmentation of three distinct retinal capillary plexuses using optical coherence tomography angiography. *Transl Vis Sci Technol*. 2019;8:57.
30. Onishi AC, Nesper PL, Roberts PK, et al. Importance of considering the middle capillary plexus on OCT angiography in diabetic retinopathy. *Invest Ophthalmol Vis Sci*. 2018;59:2167–2176.
31. Bonnin S, Mane V, Couturier A, et al. New insight into the macular deep vascular plexus imaged by optical coherence tomography angiography. *Retina*. 2015;35:2347–2352.
32. Provis JM. Development of the primate retinal vasculature. *Prog Retin Eye Res*. 2001;20:799–821.
33. Bagherinia H, Knighton RW, De Sisternes L, et al. A fast method to reduce decorrelation tail artifacts in OCT angiography. *Invest Ophthalmol Vis Sci*. 2017;58:643.
34. Bennett AG, Rudnicka AR, Edgar DF. Improvements on Littmann's method of determining the size of retinal features by fundus photography. *Graefes Arch Clin Exp Ophthalmol*. 1994;232:361–367.
35. Kim AY, Rodger DC, Shahidzadeh A, et al. Quantifying retinal microvascular changes in uveitis using spectral-domain optical coherence tomography angiography. *Am J Ophthalmol*. 2016;171:101–112.
36. Hagag AM, Pechauer AD, Liu L, et al. OCT angiography changes in the 3 parafoveal retinal plexuses in response to hyperoxia. *Ophthalmol Retina*. 2018;2:329–336.
37. Lavia C, Bonnin S, Maule M, et al. Vessel density of superficial, intermediate, and deep capillary plexuses using optical coherence tomography angiography. *Retina*. 2019;39:247–258.
38. Yu PK, Mammo Z, Balaratnasingam C, et al. Quantitative study of the macular microvasculature in human donor eyes. *Invest Ophthalmol Vis Sci*. 2018;59:108–116.

39. Ye J, Shen M, Huang S, et al. Visual acuity in pathological myopia is correlated with the photoreceptor myoid and ellipsoid zone thickness and affected by choroid thickness thinning of MEZ and choroid in pathological myopia. *Invest Ophthalmol Vis Sci*. 2019;60:1714–1723.
40. Venkatesh R, Sinha S, Gangadharaiah D, et al. Retinal structural-vascular-functional relationship using optical coherence tomography and optical coherence tomography-angiography in myopia. *Eye Vision*. 2019;6:8.
41. Mo J, Duan A, Chan S, et al. Vascular flow density in pathological myopia: an optical coherence tomography angiography study. *BMJ Open*. 2017;7:e013571.
42. Wang X, Kong X, Jiang C, et al. Is the peripapillary retinal perfusion related to myopia in healthy eyes? A prospective comparative study. *BMJ openOpen*. 2016;6:e010791.
43. Yu DY, Cringle SJ. Oxygen distribution and consumption within the retina in vascularised and avascular retinas and in animal models of retinal disease. *Prog Retin Eye Res*. 2001;20:175–208.
44. Bazzazi N, Akbarzadeh S, Yavarikia M, et al. High myopia and diabetic retinopathy: a contralateral eye study in diabetic patients with high myopic anisometropia. *Retina*. 2017;37:1270–1276.
45. Chao DL, Lin SC, Chen R, et al. Myopia is inversely associated with the prevalence of diabetic retinopathy in the South Korean population. *Am J Ophthalmol*. 2016;172:39–44.
46. Fu Y, Geng D, Liu H, et al. Myopia and/or longer axial length are protective against diabetic retinopathy: a meta-analysis. *Acta Ophthalmol*. 2016;94:346–352.
47. Linsenmeier RA, Braun RD, McRipley MA, et al. Retinal hypoxia in long-term diabetic cats. *Invest Ophthalmol Vis Sci*. 1998;39:1647–1657.
48. Yi YD, Cringle SJ, Su EN, et al. Pathogenesis and intervention strategies in diabetic retinopathy. *Clin Exp Ophthalmol*. 2001;29:164–166.
49. Nesper PL, Roberts PK, Onishi AC, et al. Quantifying microvascular abnormalities with increasing severity of diabetic retinopathy using optical coherence tomography angiography. *Invest Ophthalmol Vis Sci*. 2017;58:BIO307–BIO315.